Plant Molecular Biology (2006) 61:47–62
DOI 10.1007/s11103-005-5966-9

Spatial organisation of four enzymes from *Stevia rebaudiana* that are involved in steviol glycoside synthesis

Tania V. Humphrey, Alex S. Richman, Rima Menassa and Jim E. Brandle*
*Agriculture and Agri-Food Canada, Southern Crop Protection and Food Research Centre, 1391 Sandford St., London N5V 4T3, Ont., Canada (*author for correspondence; e-mail brandleje@agr.gc.ca)*

Received 20 June 2005; accepted in revised form 12 December 2005

Key words: cytochrome P450, diterpene, gibberellin, kaurene oxidase, metabolic engineering, UDP-glucosyltransferase

Abstract

The sweet steviol glycosides found in the leaves of *Stevia rebaudiana* Bert. are derived from the diterpene steviol which is produced from a branch of the gibberellic acid (GA) biosynthetic pathway. An understanding of the spatial organisation of the two pathways including subcellular compartmentation provides important insight for the metabolic engineering of steviol glycosides as well as other secondary metabolites in plants. The final step of GA biosynthesis, before the branch point for steviol production, is the formation of (−)-kaurenoic acid from (−)-kaurene, catalysed by kaurene oxidase (KO). Downstream of this, the first committed step in steviol glycoside synthesis is the hydroxylation of kaurenoic acid to form steviol which is then sequentially glucosylated by a series of UDP-glucosyltransferases (UGTs) to produce the variety of steviol glycosides. The subcellular location of KO and three of the UGTs involved in steviol glycoside biosynthesis was investigated by expression of GFP fusions and cell fractionation which revealed KO to be associated with the endoplasmic reticulum and the UGTs in the cytoplasm. It has also been shown by expressing the *Stevia* UGTs in *Arabidopsis* that the pathway can be partially reconstituted by recruitment of a native *Arabidopsis* glucosyltransferase.

Introduction

The leaves of the perennial herb *Stevia rebaudiana* Bert. accumulate large quantities of intensely sweet compounds known as steviol glycosides. Although their biological function is unclear, they have commercial significance for use as high potency sweeteners. In addition, recent clinical studies suggest that stevioside can reduce blood glucose levels in Type II diabetics and can reduce blood pressure in mildly hypertensive patients (Hsieh *et al.*, 2003; Gregersen *et al.*, 2004). The steviol glycosides are closely related to the gibberellins with which they share part of their biosynthetic pathway. In *Stevia*, (−)-kaurenoic acid, an intermediate in gibberellic acid (GA) biosynthesis, is converted into the tetracyclic diterpene steviol, which then proceeds through a multi-step glucosylation pathway to form the various steviol glycosides (Figure 1). The steviol glycoside biosynthetic pathway is a particularly interesting digression from the ubiquitous plant metabolic pathway for GA biosynthesis because it is extremely productive. Steviol glycosides can accumulate in leaves at concentrations as high as 20% of the dry weight (Brandle *et al.*, 1998), which is approximately 10,000 times higher than the concentration of GA_{20} found in *Stevia* leaves (Alves and Ruddat, 1979). Given that steviol and GA share common steps in their biosynthesis, the means by which

Stevia segregates the two is of interest from both a biological and a metabolic engineering standpoint.

Like all diterpenes, both GA and steviol are synthesised from the precursor geranylgeranyl diphosphate, which is formed by the deoxyxylulose 5-phosphate pathway. The activity of two different terpene cyclases (−)-copalyl diphosphate synthase (CPS) and (−)-kaurene synthase (KS) result in the formation of (−)-kaurene which is then oxidised in a three step reaction by (−)-kaurene oxidase (KO) to form (−)-kaurenoic acid (Figure 1). These enzymes from the GA biosynthetic pathway have been identified and characterised from a number of plant species including *Stevia* (reviewed in Richman *et al*., 1999; Hedden and Phillips, 2000).

Kaurene oxidase is an enzyme of the cytochrome P450 family that catalyses the three step oxidation of (−)-kaurene to form (−)-kaurenoic acid. In *Stevia* leaves, (−)-kaurenoic acid is then hydroxylated to form steviol (Kim *et al*., 1996) although neither the enzyme or the gene responsible for this reaction have yet been identified. Steviol is then glucosylated by a series of UDP-glucosyltransferases (UGTs), three of which have recently been identified and characterised (UGT85C2, UGT74G1 and UGT76G1; Richman *et al*., 2005).

UDP-glucosyltransferases catalyse the transfer of a glucose molecule to an acceptor molecule thus altering its solubility, activity, toxicity or transport. In plants, the variety of acceptor molecules include hormones, xenobiotics and innumerable secondary metabolites. Given the existence of thousands of acceptors, and only about 100 different UGTs in any given plant, the idea of one enzyme for one substrate is questionable and some degree of multifunctionality must exist (Schwab, 2003). Indeed, many UGTs have demonstrated affinity for a range of different substrates although more recent evidence, which holds true also for the *Stevia* UGTs, suggests that they are highly regiospecific and recognise a particular substructure of the acceptor molecule rather than the molecule in its entirety (Hansen *et al*., 2003; Lim *et al*., 2003; Achnine *et al*., 2005; Richman *et al*., 2005).

Unlike their mammalian counterparts, which are localised to the ER membrane, most plant UGTs are predicted to be soluble cytoplasmic enzymes although this is supported by experimental evidence for only a few plant UGTs (e.g. Yazaki *et al*., 1995; Wang and Ellis, 1998; Achnine

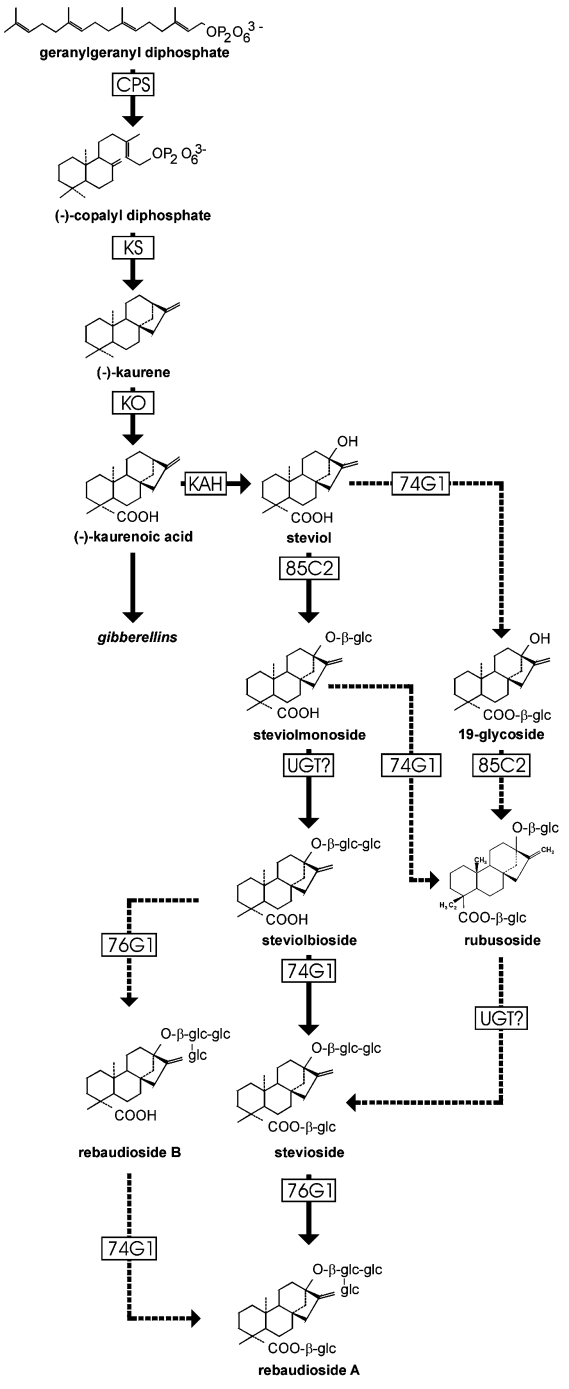

Figure 1. Biosynthetic pathway of the steviol glycosides. Dotted lines indicate steps of the pathway that are catalysed by the enzymes *in vitro* but may not be favoured *in vivo*. Abbreviations: CPS, copalyl diphosphate synthase; KS, kaurene synthase; KO, kaurene oxidase; KAH, kaurenoic acid oxidase; UGTs are abbreviated to their numerical identifiers.

et al., 2005). Given at least some degree of substrate promiscuity, it does not seem favourable for all UGTs and all potential substrates to exist in a freely diffusing cytoplasmic solution. Therefore, in addition to substrate specificity, various mechanisms such as partitioning into subcellular compartments and/or metabolic channelling may underlie the regulation of the multitude of glucosylation reactions.

One of the best studied plant secondary metabolic systems is the phenylpropanoid pathway, which produces a variety of important secondary metabolites from the amino acid precursor phenylalanine. Multiple branches of this pathway involve a number of soluble enzymes as well as membrane anchored cytochrome P450s. Phenylalanine ammonia-lyase (PAL) and cinnamate 4-hydroxylase (C4H) are two enzymes in the central pathway and both have been shown to be co-localised at the endoplasmic reticulum where metabolic channelling of intermediates occurs (Burbulis and Winkel-Shirley, 1999; Rasmussen and Dixon, 1999; Achnine *et al.*, 2004). Similarly, in sorghum, the cyanogenic glycoside dhurrin is formed from the amino acid tyrosine in a pathway catalysed by two cytochrome P450s and a soluble UGT. These apparently form a loosely associated complex anchored to the ER by the transmembrane domains of the two P450s (Neilsen and Møller, 2005). However, the formation of complexes or metabolons may not always occur. For example, the triterpene glycosyltransferase, UGT 71G1, does not appear to co-associate with membrane bound P450 enzymes that precede it in the pathway for synthesis of triterpene saponins (Achnine *et al.*, 2005).

Research into plant secondary metabolism is frequently driven by a goal of metabolic engineering in order to alter the amounts of a particular compound produced or to engineer the production of novel compounds in heterologous species. Increasingly we are learning the importance of enzyme specificity, subcellular compartmentation and sequestration of reaction products, protein–protein interactions and metabolic channelling. An understanding of these mechanisms and the role that they play in plant metabolism will provide important insight for the future engineering of a variety of secondary metabolites in plants. Steviol glycoside production in *Stevia* is one such example of an exotic secondary metabolic pathway with potential for metabolic engineering. Therefore, in addition to identifying the enzymes involved, we are also interested in examining the organisational mechanisms of this pathway. With the earlier steps known to occur in the chloroplast, and the final products accumulating in the vacuole, our goal is to shed light on how the intermediate steps are spatially organised within the cell. This current work probes the subcellular organisation of the steviol glycoside pathway by determining the localisation of several enzymes including a cytochrome P450 (KO), which is also a component of the gibberellin synthetic pathway, and three downstream UGTs specific for steviol glycoside production.

Experimental procedures

General procedures

All DNA manipulations including PCR, restriction digestion, ligation and transformation into *E. coli* XL1-Blue MRF' or *Agrobacterium tumefaciens* LBA4404 were performed by standard procedures (Sambrook and Russel, 2001). A full-length cDNA for kaurene oxidase was obtained from our EST collection (Brandle *et al.*, 2002) and used as a probe for library screening and for Southern and Northern hybridisation which were performed as described previously (Richman *et al.*, 1999). A *Stevia* genomic library was constructed using the Lambda DASH II/*Bam*HI kit (Stratagene, La Jolla, CA) according to the manufacturer's instructions. Positive clones were sequenced using the GPS-1 Genome Priming System (New England BioLabs, Beverly, MA) and contigs assembled using SeqMan II software (DNAStar, Madison, WI). The procedures used to compare relative expression of copalyldiphosphate synthase (CPS), kaurene synthase (KS), kaurene oxidase (KO) and three UDP-glucosyltransferases (UGT) were those outlined in Richman *et al.* (2005).

In vitro *functional assay of kaurene oxidase activity*

The full-length *Stevia* kaurene oxidase cDNA was cloned into the pYES2/NT yeast expression vector (Stratagene, CA, USA) and induced according to the manufacturers instructions. Thirty millilitres of the expression culture was pelleted and the cells resuspended in 1.5 ml of assay buffer [100 mM

Tris–HCl (pH 7.5), 1 mM DTT, 0.5 mM NADPH, 0.5 mM FAD] with 200 μg of kaurene. The negative control, pYES2/NT-lacZ, was run in parallel. Reactions were incubated overnight at 30 °C and 150 rpm and extracted once with 500 μl hexane and two times 500 μl with ethyl acetate. The pooled extracts were dried under a stream of N_2 at room temperature. Samples were derivatized (methylated), and products resolved using GC-MS as described in Richman *et al.* (1999). Selected ion monitoring was used for analysis of the diterpenes: (−)-kaurene, m/z 272; methyl kaurenoic acid, m/z 316. Electron impact spectra were also recorded. The samples were compared to authentic standards of methyl kaurenoic acid and (−)-kaurene which was a gift from Dr Rodney Croteau.

Plasmid construction

GT-GFP fusions were constructed using bridging PCR with partially overlapping primers. Restriction sites were added to primer sequences to facilitate cloning into plant transformation vectors. Bridging PCR was performed in two steps, the UGT sequence was amplified from a previously cloned cDNA template (Richman *et al.*, 2005) using a 5′ homologous primer and a 3′ primer consisting of the last 15 nt of the UGT coding region fused in frame to the first 15 nt of the GFP coding region. GFP was amplified from the plasmid pEGAD (Cutler *et al.*, 2000) with a 5′ primer containing the last 15 nt of the UGT coding region fused to the first 15 nt of the GFP coding region and a 3′ homologous primer. The subsequent products were added together in a second reaction performed using the UGT 5′ primer and the GFP 3′ primer. PCR was performed using the high fidelity Herculase enzyme (Stratagene, CA, USA) and a minimum number of cycles to reduce the likelihood of PCR errors. Fusion products were cloned directly into pGEMT-Easy (Promega, USA) and fully sequenced to confirm their integrity then excised and subcloned into the pBIN19-derived plant expression vector, pCaMter X which contains the dual enhanced CaMV 35S promoter (Laurian Robert, pers. comm.). The CFP and YFP vectors were similarly constructed using the codon optimised variants ECFP and EYFP, respectively (BD Biosciences, NJ, USA). High fidelity PCR was used to add the HDEL ER retention signal to the above mentioned YFP construct. A 3′ primer containing a 14 base overlap to YFP with additional sequences coding for the HDEL motif was used along with a 5′ primer homologous to YFP. Cloning and sequence verification were performed as above.

GFP imaging

GFP constructs were bombarded into onion bulb epidermis or tobacco seedling leaves as described previously (Brown *et al.*, 1994) and transient expression visualised 24 h later. Constructs were also transformed into *Arabidopsis* (Columbia) using the simplified floral dip protocol (Clough and Bent, 1998). Transgenic seedlings were selected on kanamycin at 50 μg/ml and transplanted to soil. Young leaf tissue was mounted in water for visualisation by confocal microscopy. Fluorescent images were collected using a Leica TCS SP2 inverted confocal microscope equipped with a 63× water immersion objective and Leica Confocal Software. For GFP imaging, samples were excited with the 488 nm laser line, and emissions collected between 500 and 554 nm and for chlorophyll autofluorescence between 619 and 674 nm. CFP was excited at 458 nm and emission was collected between 463 and 508 nm and YFP was excited at 514 nm and emission collected between 525 and 600 nm.

Stevia *protein extractions*

Field grown *Stevia* leaves were harvested and frozen in liquid nitrogen and stored at −80 °C for processing at a later date. Leaf tissue (10 g) was ground to a fine powder in liquid nitrogen then ground further with acid washed sand in 100 ml of freshly prepared, ice-cold extraction buffer (0.2 M potassium phosphate buffer pH 7.5, 5 mM $MgCl_2$, 10 mM ethylenediaminetetraacetic acid (EDTA), 0.2 M sodium tetraborate, 2% polyvinylpolypyrrolidone (PVPP), 1% polyvinylpyrrolidone (PVP), 20 mM β-mercaptoethanol, 2 mM 1,4-dithio-DL-threitol (DTT), 3 mg/ml sodium ascorbate, 1 mg/ml leupeptin and 1 mM phenylmethylsulphonyl fluoride (PMSF). Extract was filtered through two layers of Miracloth (Calbiochem, EMD Biosciences, USA) and cellular debris was pelleted by centrifugation at 10,000 × g for 15 min at 4 °C. Supernatant was then subjected to ultracentrifugation at 100,000 × g for 1 h at 4 °C to pellet membranes. For protein blot analysis, membranes were resuspended in 1 ml membrane

lysis buffer containing 50 mM Tris–Cl pH 7.2, 150 mM NaCl, 1 mM β-mercaptoethanol, 5 mM DTT, 0.6% IGEPAL CA630 (Sigma), 0.5% 3-[(3-Cholamidopropyl)dimethylammonio]-1-propanesulfonate (CHAPS) and protease inhibitors. For activity assays, membranes were resuspended in extraction buffer lacking the sodium tetraborate, PVPP, PVP and sodium ascorbate, supplemented with 10% glycerol. Soluble proteins from the supernatant were precipitated with ammonium sulphate and the useful fraction collected between 25% and 65% saturation. Precipitated proteins were resuspended in a minimal volume of phosphate buffered saline (PBS) and either used directly for protein blot analysis or desalted on a PD-10 sephadex G25 column (Amersham Biosciences, UK) equilibrated with PBS.

Glucosyltransferase activity assays

The UGT activity assays were carried out using 300 μg of *Stevia* soluble or membrane protein fractions or 30 μg of *Arabidopsis* total protein extract. Reaction conditions and analysis by thin layer chromatography were performed as described previously (Richman *et al*., 2005).

Antibody production and protein gel blot analysis

Recombinant UGT85C2, UGT74G1 and UGT76G1 protein was produced in *E. coli* as described previously (Richman *et al*., 2005). The recombinant protein was found predominantly in the insoluble fraction which was resuspended in 1 ml of sonication buffer (2 M urea, 20 mM Tris–Cl, 0.5 M NaCl, 2% Triton-X-100, pH 8.0) and sonicated followed by centrifugation as before. Recombinant UGT protein was purified from the inclusion bodies by washing three times in 10 ml of sonication buffer then three times in 10 ml of wash buffer (20 mM Tris–Cl, 0.1 M NaCl, 0.1% sodium dodecyl sulfate (SDS), pH 8.0) using a syringe with an 18 gauge needle to thoroughly resuspend the inclusion bodies followed by centrifugation. The final pellet containing essentially pure recombinant protein was dissolved in 10 ml of solubilisation buffer containing 8 M urea, 20 mM Tris–Cl and 0.15 M NaCl with pH adjusted to 8.0. The protein was quantified and checked for purity using SDS-PAGE and then diluted 50- to 100-fold in PBS to a final concentration of 500 ng/μl.

Antibodies were raised in rabbits, one for each of the three UGTs. Inoculation was carried out subcutaneously at four injection sites. Protein (125 μl per injection site) was mixed with complete Freund's adjuvant for primary inoculation and incomplete Freund's adjuvant for the remainder. Inoculation was repeated at 2 week intervals for a period of 2 months. Removal of non-specific antibodies was carried out by negative purification on PVDF membranes (Bio-Rad, CA, USA) essentially as described (Benet and Van Cutsem, 2002). Bacterial cultures of two of the UGTs were pooled and used to purify the antiserum from the third. Total insoluble protein from 1 l of bacterial culture was collected as described above and resuspended in 3 ml of solubilisation buffer. The entire protein extract was loaded onto two mini-gels (Bio-Rad, CA, USA),transferred to PVDF membranes and allowed to dry before blocking overnight in 10% skim milk powder/Tris buffered saline (TBS). Antiserum was diluted to 1:500 in 3% BSA/TBS and 10 ml was incubated with both blots overnight at 4 °C with gentle agitation. Remaining antiserum was collected and elimination of cross reactivity was confirmed by western.

Samples (150 μg) of each of the ammonium precipitated soluble fraction and the membrane fraction of *Stevia* leaf extracts were run on non-denaturing polyacrylamide gels and transferred to nitrocellulose membranes. Blocking was carried out by incubating blots overnight at 4 °C in blocking solution containing 5% skim milk in TBS. Blots were incubated with negatively purified antisera diluted in blocking solution at the following dilutions: antiUGT76G1 at 1:80,000 and antiUGT85C2 at 1:30,000 followed by incubation with a Goat anti-rabbit IgG coupled to horseradish peroxidase secondary antibody (Bio-Rad, CA, USA) at a 1:3000 dilution. Bands were visualised on Kodak film using the ECL chemiluminescence assay kit (Amersham Biosciences, UK) according to the manufacturer's instructions.

Results

Cloning and characterisation of Stevia *kaurene oxidase*

A full-length KO cDNA (SrKO1) was identified in a collection of *Stevia* leaf ESTs, by its homology to

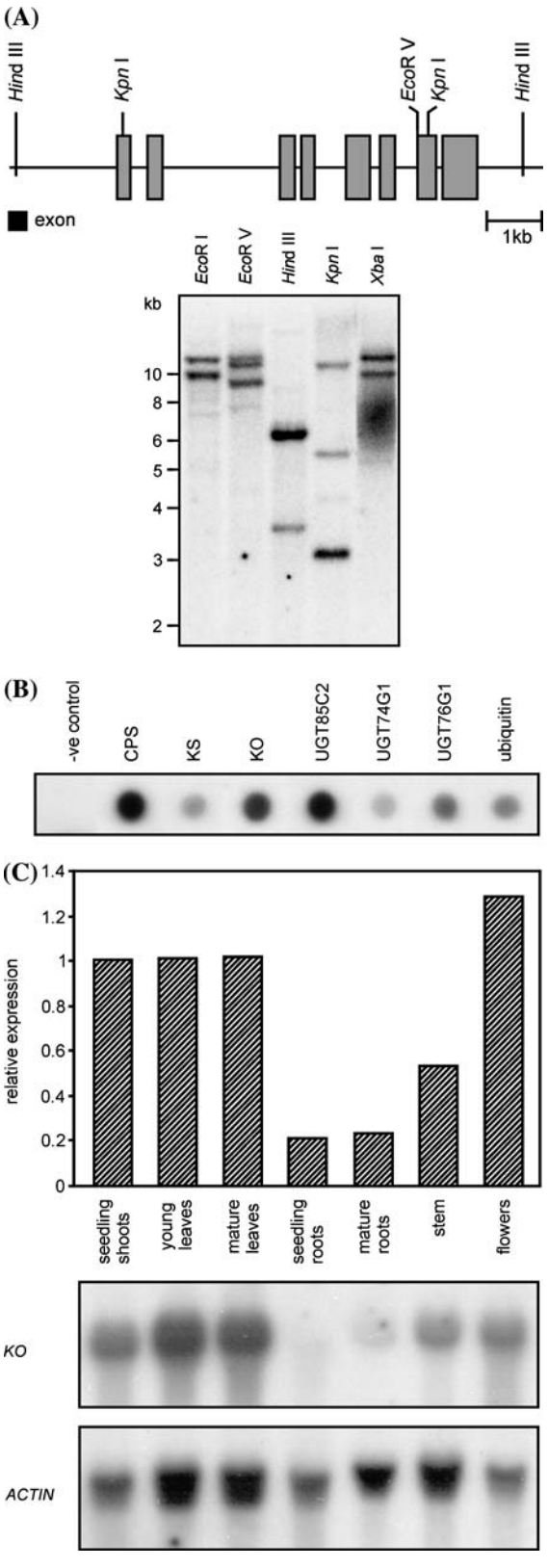

Figure 2. Gene structure and expression analysis of *Stevia* kaurene oxidase. (A) Genomic structure of KO indicating introns and exons and Southern blot analysis with banding pattern confirming the presence of at least two intact copies of KO. (B) DNA dot blot showing relative expression levels in mature leaves of several genes involved in steviol glycoside synthesis. (C) Northern blot analysis of KO gene expression in *Stevia* using 10 μg of total RNA extracted from various plant tissues. To simplify this comparison a bar graph is presented indicating expression levels standardised to actin.

other plant kaurene oxidases (Brandle *et al*., 2002) and used as a probe to screen a *Stevia* genomic DNA library using high stringency washes. Several clones were isolated, which assembled into two independent genomic fragments containing two copies of KO (SrKO1 and SrKO2) with 99.5% identity to each other but in different genomic contexts. Sequence analysis of the coding regions of the KO ESTs and genomic clones revealed only occasional single nucleotide variation although the translated amino acid sequences were conserved; the non-coding regions were also highly conserved. At the amino acid level the *Stevia* KO1 sequence has 58% identity (87% similarity) to the *Arabidopsis* AtKO1 and has been grouped in the same gene family and assigned the name CYP701A5 (http://www.drnelson.utmem.edu/CytochromeP450.html); GenBank accessions AY364317 (SrKO1, mRNA), DQ200952 (SrKO1, gDNA), AY995178 (SrKO2, gDNA). The genomic structure of the two KO genes was identical and consisted of eight exons and seven introns (Figure 2A). In addition to the full-length version of the gene, one of the genomic fragments contained an additional copy, approximately 4.8 kb downstream which is truncated after the first four exons. Southern analysis of the restriction fragments from *Stevia* genomic DNA using the full-length SrKO1 cDNA as a probe was consistent with the presence of two complete and one partial copy of KO in the *Stevia* genome (Figure 2A).

A DNA dot blot of several functionally characterized glycoside pathway genes was hybridised with ^{32}P labelled cDNA reverse transcribed from leaf total RNA (Figure 2B). This comparison showed varying levels of expression in leaves with CPS and UGT85C2 being the most highly expressed and KO showing relatively moderate expression. By comparison, expression of all of the genes in roots was low (data not shown). Further

analysis of KO1 gene expression was conducted using northern blot analysis and standardised for loading against *Stevia* actin (Figure 2C). In that experiment KO1 transcript was detectable in all tissues examined with the highest expression in leaves and flowers and the lowest in roots.

To test for functionality, the coding region of *Stevia* KO1 was cloned into the pYES2/NT vector for recombinant expression in *Saccharomyces cerevisiae*. Cytochrome P450 activity assays were conducted using the recombinant yeast extract with (−)-kaurene as a substrate. Analysis of the hexane/ethyl acetate extract of the reaction mixture using gas chromatography-mass spectrometry (GC-MS) with single ion monitoring at m/z 316 (molecular ion of methyl kaurenoic acid) revealed a peak at the retention time of the methyl kaurenoic acid standard (Figure 3), indicating conversion had occurred. A parallel experiment with recombinant lacZ protein (pYES2/NT-lacZ) revealed a single peak at the retention time of (−)-kaurene indicating no conversion. This demonstrates that *Stevia* KO1 has complete catalytic activity for the three step conversion of (−)-kaurene to (−)-kaurenoic acid.

Stevia *KO is located in the endoplasmic reticulum*

Analysis of the *Stevia* KO protein sequence using the prediction programs TMHMM (Krogh *et al*., 2001) and TMpred (Hofmann and Stoffel, 1993) suggested the presence of one membrane spanning helix near the N-terminus, which is typical of the membrane anchor found at the N-terminus of most plant microsomal P450s (Werck-Reichhart *et al*., 2002). The subcellular location prediction program PSORT (Nakai and Horton, 1999) suggested that SrKO1 was localised to the membrane of the endoplasmic reticulum (ER)($p = 0.640$).

The subcellular location of SrKO1 was further investigated *in vivo* by fusing SrKO1 to the N-terminus of the enhanced GFP variant EGFP (Cormack *et al*., 1996) and putting the gene fusion under the control of the dual enhanced CaMV 35S promoter. The fusion constructs were transiently expressed in both onion epidermal cells and tobacco leaf cells by particle bombardment and fluorescing cells visualised by confocal microscopy. SrKO1-GFP fluorescence in onion cells was

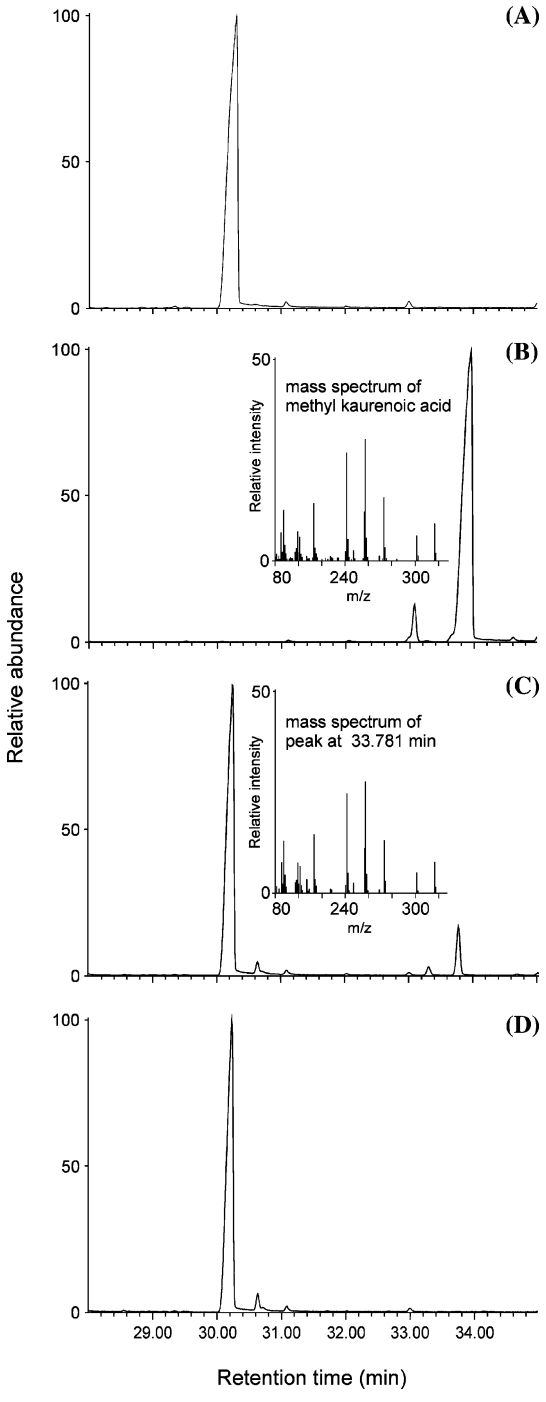

Figure 3. In vitro analysis of recombinant kaurene oxidase (KO) activity in yeast. GC-MS analysis with selected ion monitoring of diterpene products: (A) kaurene (m/z 272); (B) authentic methyl kaurenoic acid (m/z 316); (C) product of incubation of (−)-kaurene and pYES2/NT-KO expression culture; (D) product of incubation of (−)-kaurene and pYES2/NT-lacZ expression culture.

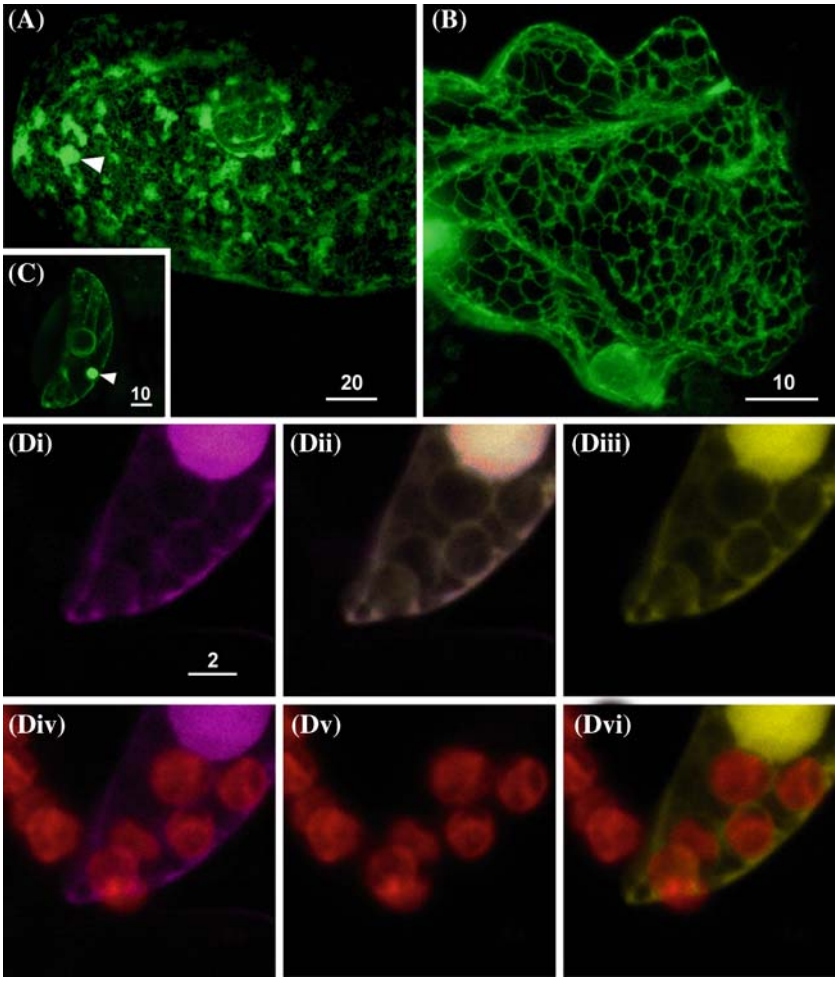

Figure 4. Expression of KO-GFP fusions in plant cells. KO-GFP fusion constructs were bombarded into onion epidermis (A), tobacco epidermal cells (B) and photosynthetic guard cells (C). Guard cells with KO-CFP (Di), YFP-HDEL (Diii), and the overlay of KO-CFP/YFP-HDEL (Dii). Chlorophyll autofluorescence (Dv) and corresponding overlays with KO-CFP (Div), YFP-HDEL (Dvi). The arrow indicates brightly fluorescing structures. Scale bars indicate size in μm.

visible as an irregular webbing pattern throughout the cell and surrounding the nucleus (Figure 4A). The distinctive reticulate pattern of the ER was very clear when the construct was expressed in tobacco epidermal cells (Figure 4B). In many of the cells, a large, extremely bright structure was visible which frequently moved, often causing blurring in the images (Figure 4C). To examine localization in photosynthetic cells SrKO1 was fused to the GFP cyan variant (CFP) and co-bombarded with the yellow variant (YFP) targeted to the ER by addition of the HDEL ER retention signal. The expression pattern for SrKO1 and YFP-HDEL were nearly identical, with the fluorescent ER network enveloping the chloroplast in both cases but with no fluorescence visible with the chloroplast itself (Figure 4D).

The glucosyltransferases involved in steviol glycoside synthesis are located in the cytosol

Homology based screening of our *Stevia* EST collection identified several candidate UGTs and, based on the *in vitro* activity of the recombinant enzymes, three were shown to be involved in steviol glycoside synthesis (Richman *et al*., 2005). In order to detect activity of the native enzymes, protein was extracted from *Stevia* leaves and separated into soluble and microsomal fractions. Both fractions were then assayed for

glucosyltransferase activity using each of the pathway intermediates as substrates in the reactions. Reaction products were separated by thin layer chromatography (TLC) and identified by comparing the calculated R_f values with a set of known standards. Some background activity was visible in the control lane with no substrate, which was probably due to glycosylation of unknown plant metabolites present in the protein extract. Activity of each of the three UGTs was found to occur exclusively in the soluble fraction of leaf extracts (Figure 5A). For most substrates more than one product was formed indicating flow of metabolites through the pathway. Under the conditions specified, TLC gave insufficient resolution to differentiate between 19-O-β-glucopyranosyl-steviol (abbreviated to 19-glycoside) and steviol monoside, both of which contain a single unit of glucose and also between steviol bioside and rubusoside, which each contain two glucose units. In these cases the reaction products were isolated from the TLC plate and identified by LC-MS. With steviol as a substrate, a small amount of both the 19-glycoside and steviol monoside were formed although the predominant product was rubusoside, small amounts of steviol bioside, stevioside and rebaudioside A were also detected. With steviol bioside, stevioside and rebaudioside B as substrates, rebaudioside A was the dominant product demonstrating that the reaction proceeded to completion. Taken together, these results clearly show activity of each of the three UGTs in the soluble fraction, as well as that of the unidentified UGT in the production of steviol bioside from steviol monoside. Despite the fact that large amounts were formed, rubusoside was not utilised as a substrate to form stevioside. The presence of UGT85C2 and UGT76G1 in the soluble fraction was further confirmed by western blot analysis using antibodies raised against each of the recombinant proteins (Figure 5B). The UGT76G1 antibodies displayed some degree of cross-reactivity which was visible as a second band of the same size as UGT85C2, which is may be due to a structural similarity between UGT76G1 and another UGT or that there may be a small protein interacting with UGT76G1. Although the activity of UGT74G1 was detectable, antibodies raised against this enzyme were either not sufficiently sensitive or the enzyme concentration was too low to allow detection in either fraction.

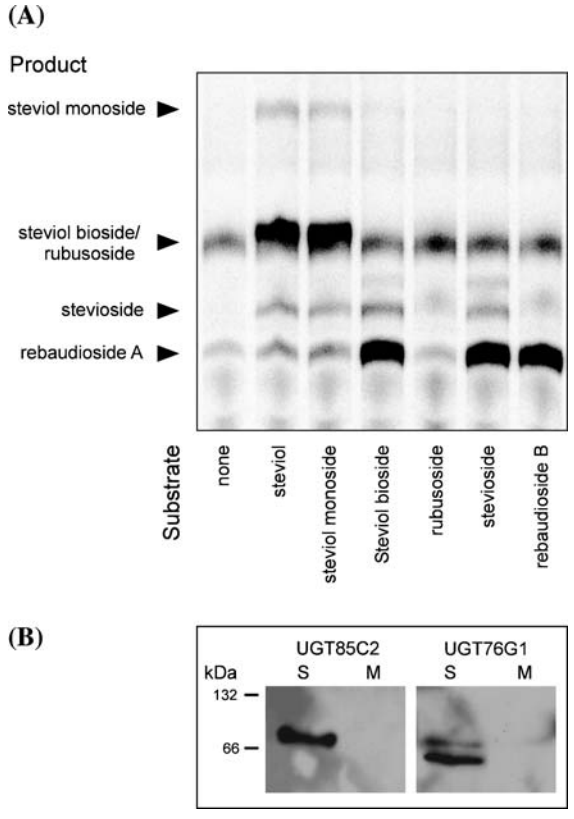

Figure 5. Glucosyltransferases in *Stevia* extracts. (A) Image of TLC separation of radiolabelled reaction products after incubation with a soluble protein fraction from *Stevia* and various substrates as indicated. (B) Western blot analysis of soluble (S) and membrane (M) protein fractions from *Stevia* using antibodies raised against UGT76G1 and UGT85C2.

Sequence analysis of the UGTs using the TMHMM protein sequence analysis program (Krogh *et al*., 2001) predicted that UGT85C2 contained an N-terminal transmembrane domain, which could indicate a membrane location. Further analysis using a number of programmes designed to predict subcellular locations for the UGTs gave variable results although all predicted at low confidence. The *in vivo* localisation of each of the UGTs was resolved using GFP fusions introduced for transient expression in onion bulb epidermis and stable expression in *Arabidopsis*.

Visualisation by confocal microscopy revealed an identical expression pattern for each of the three UGTs. In both onion and *Arabidopsis*, each of the UGT-GFP fusions displayed the diffuse fluorescence pattern characteristic of a cytoplasmic location (Figure 6). This pattern was identical to that of untargeted soluble GFP which, in addition to the cytoplasm, has a tendency to accumulate in the nucleus (Figure 6C). However, diffusion of the

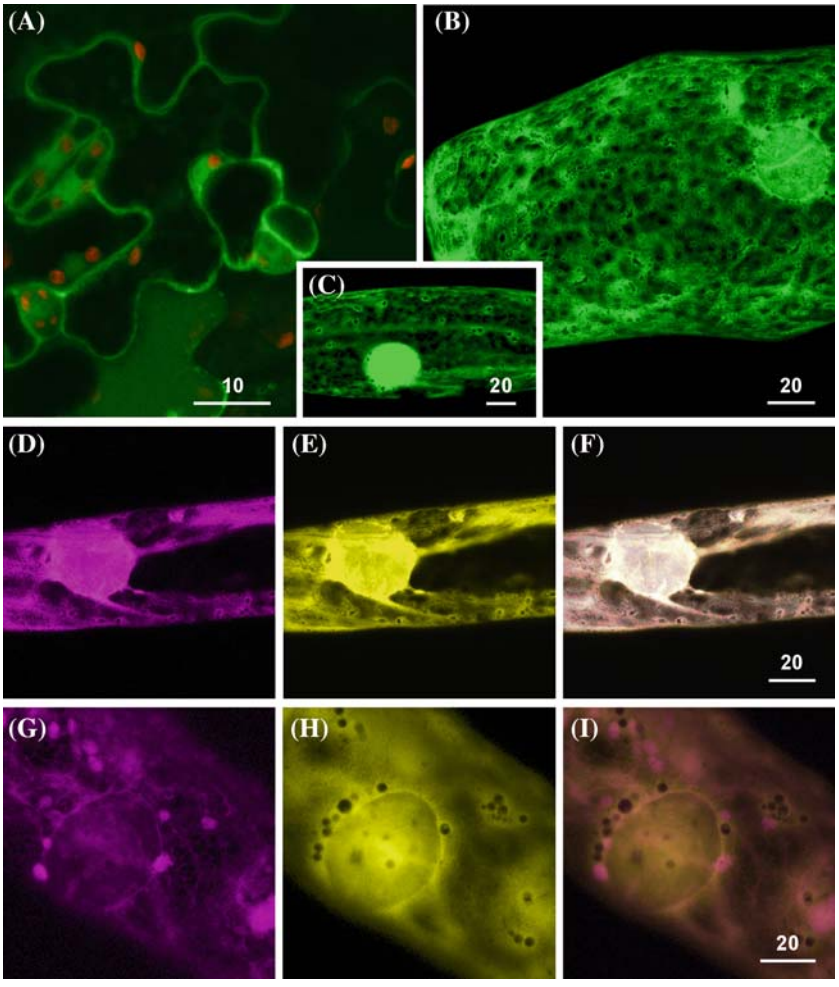

Figure 6. Expression of UGT-GFP fusions and co-expression of UGT and KO fusions in plant cells. (A) UGT74G1-GFP expression in transgenic *Arabidopsis*, image shown is an overlay of green and red chlorophyll autofluorescence channels. (B) UGT74G1-GFP fluorescence in onion epidermal cell. (C) Untargeted GFP control in onion epidermal cell. UGT74G1-CFP (D) co-expression with UGT76G1-YFP (E) in onion epidermal cell and overlay (F). Co-expresssion of KO-CFP (G) and UGT76G1-YFP (H) in onion epidermal cell and overlay (I). For clarity, CFP fluorescence (D and G) is shown in magenta and YFP fluorescence (E and H) in yellow. Co-localisation of fluorescence in overlays appears white. Scale bars indicate size in μm.

UGT-GFP fusions into the nucleus should be limited due to their larger size. Indeed, the relative intensity of the fluorescence in the nucleus compared to the cytoplasm was generally much lower for the UGT-GFP fusions than for untargeted GFP, which produced extremely bright fluorescing nuclei. The UGT-GFP fusions were excluded from chloroplasts and other subcellular organelles which are visible as small black spaces or 'bubbles' in the surrounding fluorescence. The production of intact fusion proteins of the expected size was confirmed by western blot analysis of extracts from transgenic *Arabidopsis* plants using GFP antibodies (data not shown).

In addition to the GFP fusion constructs, each of the UGTs and SrKO1 was fused to either the cyan variant; CFP or the yellow variant; YFP, under control of the dual enhanced 35S promoter for co-localisation studies. Both the CFP and YFP fusion constructs were co-bombarded into onion bulb epidermis and examined by confocal microscopy. Co-expression of each of the UGTs in combination with each other showed a diffuse fluorescence throughout the cytoplasm and nucleus. The expression pattern was identical to that seen when either of them was expressed alone (e.g. Figure 6D–F). The possibility of molecular interactions between the UGTs was

also investigated using fluorescence resonance energy transfer (FRET) analysis (data not shown) and the results demonstrated that no significant FRET occurred between the molecules. Similarly, co-expression of each of the UGTs with SrKO1 (Figure 6G–I) resulted in independent fluorescence patterns, the same as was seen for each gene expressed alone. The CFP and YFP localisation studies suggest that the UGTs are co-localised in the cytoplasm although no aggregation or molecular interaction was observed.

Stevia *UGTs act in tandem with an endogenous Arabidopsis enzyme for partial reconstitution of the pathway*

In order to establish a baseline, non-transformed *Arabidopsis* was tested for glucosyltransferase activity with each of the steviol glycoside substrates and interestingly was found to glucosylate steviol, steviol monoside and steviol bioside. The *Arabidopsis* glucosylation products were visualised by TLC (Figure 7) and identified based on comparison of their R_f values to known standards and when necessary, the 19-glycoside and steviol monoside were differentiated by LC-MS. The glucosylation product with steviol as a substrate was the 19-glycoside, no steviol monoside was detected. Steviol monoside was glucosylated to rubusoside and steviol bioside glucosylated to stevioside. The *Arabidopsis* extract showed only limited activity for the conversion of rebaudioside B to rebaudioside A (data not shown). Therefore, the non-transformed *Arabidopsis* extract glucosylated the C-4 hydroxl group of steviol and the activity resembles that of UGT74G1 from Stevia.

To confirm that the UGT-GFP fusions in *Arabidopsis* still retained their native activity, a series of glucosyltransferase assays were conducted using protein extracts from the fluorescing plants along with appropriate substrates. Each of the *Arabidopsis* UGT-YFP expressing lines was tested with the corresponding substrates on which it was expected to act (Figure 1). In all cases it was found that the fusions retained the specific activity of the native UGT and produced the expected glucosylation products. However, for UGT85C2 and UGT76G1, additional glucosylation products were generated, demonstrating an interaction between the native and heterologous UGTs for sequential glucosylation reactions (Figure 7a, b).

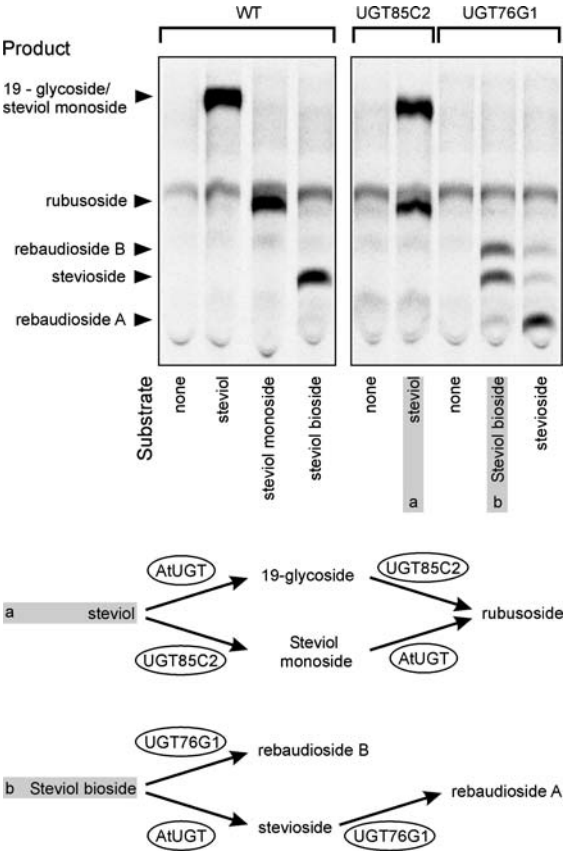

Figure 7. Steviol glucosyltransferase activity in *Arabidopsis*. Radiolabelled reaction products separated by TLC after incubation with protein extracts from non-transformed (WT) and transgenic *Arabidopsis* expressing UGT-YFP fusions. Reactions shown in A and B indicate sequential glucosylation steps involving both a native *Arabidopsis* UGT (*At*UGT) and the introduced *Stevia* UGT.

For example, when UGT85C2 was present, both the 19-glycoside and steviol monoside were formed and subsequently glucosylated to form rubusoside. Likewise, when UGT76G1 was expressed, steviol bioside was glucosylated to form rebaudioside B and stevioside. A small amount of rebaudioside A was also detected indicating an additional glucosylation step, most likely from the activity of UGT76G1 on stevioside.

Discussion

Stevia *kaurene oxidase is upregulated in mature leaves where it plays a role in steviol biosynthesis*

In studies of gibberellin synthetic enzymes in *Arabidopsis*, *Cucurbita maxima* and pea, kaurene

oxidase was found to be expressed predominantly in developing seeds and young, rapidly growing tissues with low expression levels in mature leaves (Helliwell *et al*., 1998, 2000; Davidson *et al*., 2004). In *Stevia* however, kaurene oxidase was found to be expressed in both young and mature leaf tissues. Even though kaurene oxidase was identified in our leaf EST collection as one of the most abundant transcripts, the RNA levels were lower than expected, which confirms earlier observations that gene expression does not necessarily correlate with EST representation (Brandle *et al*., 2002). In contrast to other plant species, where gene expression in leaves is extremely low, in *Stevia*, CPS, KS and KO are all highly expressed in leaves (Richman *et al*., 1999). This is consistent with the upregulation of key steps of the GA biosynthetic pathway and their recruitment for high levels of steviol glycoside production. However, the increased abundance of these enzymes does not appear to interfere with gibberellin metabolism as an important rate limiting step occurs downstream of the branch point for steviol production (Fleet *et al*., 2003).

In both *Arabidopsis* and pea, KO occurs as a single copy gene (Helliwell *et al*., 1998; Davidson *et al*., 2004) although in rice, five copies have been found (Itoh *et al*., 2004). In *Stevia* we have found that there are two copies with a third truncated copy that is probably non-functional. It seems likely that the two copies of KO have arisen as a result of a duplication event, similar to the two nearly identical copies of KS previously found in *Stevia* (Richman *et al*., 1999). It is tempting to speculate that one version of KO is utilised for GA biosynthesis and the other for steviol production although the two KO genes encode identical proteins so it is more likely that if any differential regulation occurs it would be at the level of gene expression. Analysis of upstream regulatory sequences may shed further light on this.

Spatial organisation of the steviol glycoside biosynthetic pathway

The spatial organisation of the steviol glycoside biosynthetic pathway was investigated by determining the subcellular location of several enzymes. Kaurene oxidase was of interest because of its dual role in both gibberellin and steviol synthesis and as expected from other cytochrome P450s, was found to be located on the ER. The glucosyltransferases play the major role in the latter part of the pathway producing a variety of steviol glycosides and were found to be located in the cytosol. Taken together with other evidence, our current understanding of the spatial organisation of the pathway is summarised in Figure 8.

In *Arabidopsis*, kaurene synthase was found to be located in the chloroplast stroma (Sun and Kamiya, 1994; Helliwell *et al*., 2001) and it seems likely that in *Stevia*, KS is also a stromal protein as this was predicted at a very high probability (0.938) by the subcellular location prediction program PSORT (Nakai and Horton, 1999). KS produces the reaction intermediate (−)-kaurene which has a low polarity and is therefore likely to partition into membranes. The next step of the pathway is catalysed by KO and expression of a *Stevia* KO-GFP fusion in plant cells strongly suggests that the protein is targeted to the endoplasmic reticulum. The predicted membrane anchor and similarity to other cytochrome P450s further suggest that it is embedded within the membrane. (−)-Kaurene must then move from its site of synthesis in the chloroplast stroma, out through the membranes and into the ER membrane where it would be accessible to KO. A

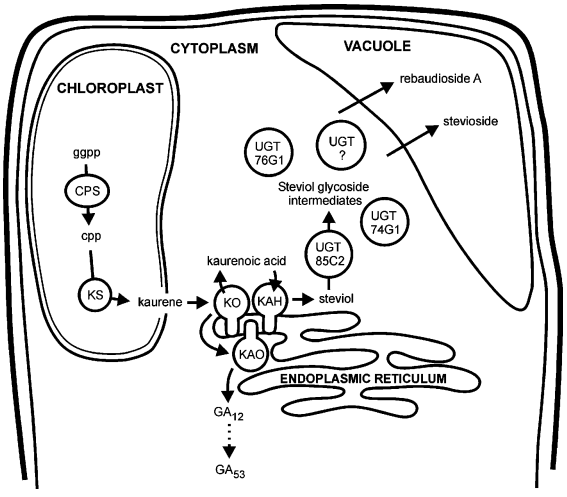

Figure 8. Subcellular organisation of the steviol glycoside biosynthetic pathway. Schematic of a plant cell showing early steps congruent with GA biosynthesis, occurring in the chloroplast. The *Stevia* KO was shown to be located on the ER which is also the proposed location for kaurenoic acid hydroxylase. Downstream production of intermediates occurs via cytoplasmically located UGTs with the glycosides stevioside and rebaudioside A accumulating in the vacuole.

previous report located *Arabidopsis* KO on the outer membrane of the chloroplast although there was also some evidence suggesting an additional ER location (Helliwell *et al*., 2001). These authors suggested that a chloroplastic KO would provide the necessary link between chloroplast and ER located steps of gibberellin synthesis, but exactly how this would occur is still not known. In this current work, co-expression of a *Stevia* KO:CFP fusion and YFP-HDEL resulted in distinctive ER fluorescence with no visible fluorescence in the chloroplast suggesting that in *Stevia* KO may be found predominantly on the ER membrane with little, if any expression in the chloroplasts. This observation is further supported by results from the chloroplast transit peptide prediction program, ChlorP (Emanuelsson *et al*., 1999), which predicted a chloroplast target peptide for AtKO1, but not for SrKO1 nor for KO proteins from *Oryza sativa*, *Hordeum vulgare*, *Fragaria grandiflora*, *Pisum sativum*, *Cucurbita maxima*.

The presence of the UGT-GFP fusions in the nucleus was unexpected due to the general assumption that UGTs are operationally soluble enzymes found in the cytoplasm. However, Grebenok *et al*. (1997) found that fusions needed to be at least 100 kDa to limit nuclear penetration. Furthermore, the presence of large cytoplasmic protein GFP fusions in the nucleus has been reported before and was shown to be caused by passive diffusion, with the effect accumulating over time (Kudo *et al*., 1998; Haasen *et al*., 1999). This is consistent with our observation that the nuclei in the GFP controls were significantly brighter than the nuclei in the UGT-GFP fusion plants whereby GFP alone can diffuse into the nucleus much more readily than the larger fusions. Alternatively the protein may contain both nuclear localisation and export signals (Nagatani and Matsushita, 2002) although this does not seem likely given the role of the UGTs in secondary metabolism and the absence of known nuclear localization signals from the protein sequence. Likewise, the extremely bright, solid structures that were frequently observed in the SrKO1-GFP expressing cells, in both tobacco and onion are of an unknown nature (Figure 4). It is interesting that similar structures have also been observed with a P450 from poplar, cinnamate 4-hydroxylase, when GFP fusions were over-expressed in *Arabidopsis* (Ro *et al*., 2001) and with isoflavone 3′ hydroxylase over-expressed in *Medicago truncatula* (Liu *et al*., 2003). Current thinking is that the structures are simply protein aggregates.

Expression of *Stevia* UGT-GFP fusions indicated a cytoplasmic location, at least when expressed in onion or *Arabidopsis* cells and this was confirmed by the presence of the protein in soluble extracts from *Stevia*. Even though most plant UGTs are predicted to occur in the cytoplasm, experimental evidence is varied. Cell fractionation studies have shown a number of UGTs to be localised to membranes (Loffelhardt and Kopp, 1981; Kalinowska and Wojciechowski, 1987; Warnecke and Heinz, 1994) although several other studies using cell fractionation, immunolocalisation or expression of GFP fusions have reported UGTs in the cytoplasm (Blume *et al*., 1979; Schmid *et al*., 1982; Yazaki *et al*., 1995; Dean *et al*., 2003; Achnine *et al*., 2005). The results from both our cell fractionation studies and GFP fusions strongly suggest that UGT85C2, UGT74G1 and UGT76G1 are located in the cytoplasm. Both UGT76G1 and UGT74G1 are necessary to produce stevioside and rebaudioside A, which ultimately accumulate in the vacuole. This differential localisation of glycosyltransferases in the cytoplasm with accumulation of products in the vacuole has also been reported for salicylic acid conjugates in soybean and indican in the indigo plant (Minami *et al*., 2000; Dean *et al*., 2003). As the UGTs are not physically associated with the vacuole, there may be other factors involved such as transfer or carrier proteins.

Metabolic channeling

Despite the accumulation of extremely large quantities of stevioside and rebaudioside A in *Stevia* leaves, the earlier intermediates are present at very low concentrations (J. Brandle, unpublished results). This is in contrast to the results from the *Stevia* UGT activity assays performed with soluble protein extracts in which all of the intermediates are represented, most notably, large amounts of rubusoside (Figure 5). Despite the large quantities formed, we found that extracts were unable to glucosylate rubusoside, as previously reported (Shibata *et al*., 1995), suggesting that the formation of rubusoside is an unproductive branch of the pathway and not likely to occur *in vivo*. Therefore, there must be a mechanism within the

cell to prevent rubusoside from being formed or more specifically to prevent UGT74G1 from accessing steviol monoside as a substrate. This mechanism is disrupted by the extraction process, although it is probably not based on segregation into different subcellular compartments, as all the UGTs were found in the cytoplasm.

The evidence from our activity assays suggests metabolic channelling, but so far we have found no evidence for the existence of a UGT enzyme complex. Western analysis of leaf protein extracts subjected to non-denaturing PAGE showed no increase in expected product size which would indicate complex formation with other proteins (Figure 5). Co-expression of varying combinations of KO-GFP and UGT-GFP fusions in plant cells had no effect on the cellular distribution of the UGTs. Also, FRET analysis using CFP and YFP fusions as well as specific yeast-two-hybrid interaction assays showed no significant interaction between any of the UGTs (data not shown), although these techniques have previously been reported to show interaction between enzymes in the phenylpropanoid and flavonoid pathways (Burbulis and Winkel-Shirley, 1999; Achnine *et al.*, 2004). If there is any interaction between the UGTs, it is most likely weak and/or transient. Alternatively, metabolon formation may require the presence of additional components such as kaurenoic acid hydroxylase. Or, given the apparent channeling of steviol monoside, the interaction may occur only between UGT85C2 and the unidentified UGT. Our results so far favour a model of steviol glycoside synthesis where the UGTs are found in the cytosol, but there is some evidence for metabolic channeling and an ER-based enzyme complex remains a possibility.

Pathway engineering

We have shown that an *Arabidopsis* protein extract is able to glucosylate steviol and other intermediates of the steviol glycoside pathway, mimicking the action of UGT74G1 from *Stevia*. Even though there are over 100 predicted *Arabidopsis* UGTs, this is a very specific pattern of activity resulting from glucosylation of each of the substrates only at the C-19 position. Therefore it is likely that only a single glucosyltransferase is responsible. This same activity was also detected in tobacco extracts suggesting that this UGT may be a ubiquitous plant enzyme whose native substrate could be any number of structurally similar plant metabolites, most notably the gibberellins.

The ability of *Arabidopsis* to glucosylate steviol is perhaps not surprising given that glucosylation is a ubiquitous mechanism that plants use for protection against toxic xenobiotics (Kristensen *et al.*, 2005). However, in this instance the glycoside formed is a useful pathway intermediate and we have been able to exploit this native activity in tandem with the *Stevia* UGTs to produce sequential products in the steviol glycoside pathway. The functional reconstitution of part of the steviol glycoside synthetic pathway in *Arabidopsis* demonstrates the recruitment of a native plant enzyme to a novel pathway, which could be extremely useful for metabolic engineering. Although there have been a number of reports of unexpected processing of novel secondary metabolites in plants, most are considered undesirable side effects or metabolic cross talk. The beneficial recruitment of native plant enzymes to a novel pathway has previously been reported in Golden Rice, which was engineered for β-carotene synthesis (Ye *et al.*, 2000). However, in this example the novelty comes from engineering a metabolic pathway in new cell types within the same species whereas the production of steviol glycosides in *Arabidopsis* is a completely novel pathway which occurs in very few species other than *Stevia rebaudiana*.

The *Stevia* UGTs isolated so far, as well as the native plant UGT have all demonstrated regiospecificity in that they always add a glucose onto the same site on the steviol skeleton but at the same time can act on more than one substrate in the pathway (Figure 1). This means that there is potentially more than one way to assemble the final products, which adds flexibility to metabolic engineering efforts. In addition, the ability to recruit native enzymes for steviol glycoside synthesis reduces the need for engineering all pathway components giving greater flexibility in choosing a metabolic engineering approach. The same may be found true in other plant metabolic pathways involving glucosyltransferases.

In conclusion, the recruitment of GA synthesis enzymes and the up-regulation of their expression in leaves was a key step in the evolution of diterpene metabolism in *Stevia*. Subcellular localisation of KO, which has a dual role in both steviol and gibberellin biosynthesis and three of the

downstream glucosyltransferases has given us considerable insight into the organisation of this pathway within the cell. Further work will be necessary in order to fill in some of the gaps in our understanding, specifically the role of metabolic channelling and transporter proteins both in this and other secondary metabolic pathways.

Acknowledgements

We gratefully acknowledge John Hendel and Bob Pocs for assistance with HPLC and Ralph Chapman for the LC-MS analysis. We are grateful also to Katrina Haasen for assistance with transgenic plant lines.

References

Achnine, L., Blancaflor, E.B., Rasmussen, S. and Dixon, R.A. 2004. Colocalization of L-phenylalanine ammonia-lyase and cinnamate 4-hydroxylase for metabolic channeling in phenylpropanoid biosynthesis. Plant Cell 16: 3098–3109.

Achnine, L., Huhman, D.V., Farag, M.A., Sumner, L.W., Blount, J.W. and Dixon, R.A. 2005. Genomics-based selection and functional characterization of triterpene glycosyltransferases from the model legume *Medicago truncatula*. Plant J. 41: 875–887.

Alves, L.M. and Ruddat, M. 1979. The presence of gibberellin A_{20} in *Stevia rebaudiana* and its significance for the biological activity of steviol. Plant Cell Physiol. 20: 123–130.

Benet, C. and Van Cutsem, P. 2002. Negative purification for the selection of specific antibodies from polyclonal antisera. BioTechniques 33: 1050–1054.

Blume, D.E., Jaworski, J.G. and McClure, J.W. 1979. Uridinediphosphate-glucose: isovitexin-7-O-glucosyltransferase from barley protoplasts: subcellular localisation. Planta 146: 199–202.

Brandle, J.E., Richman, A., Swanson, A.K. and Chapman, B.P. 2002. Leaf ESTs from *Stevia rebaudiana*: a resource for gene discovery in diterpene synthesis. Plant Mol. Biol. 50: 613–622.

Brandle, J.E., Starratt, A.N. and Gijzen, M. 1998. *Stevia rebaudiana*: its agricultural, biological, and chemical properties. Can. J. Plant Sci. 78: 527–536.

Brown, D.C.W., Tian, L., Buckley, D.J., Lefebvre, M., McGrath, A. and Webb, J. 1994. Development of a simple particle bombardment device for gene transfer into plant cells. Plant Cell Tissue Organ Cult. 37: 47–53.

Burbulis, I.E. and Winkel-Shirley, B. 1999. Interactions among enzymes of the *Arabidopsis* flavonoid biosynthetic pathway. Proc. Natl. Acad. Sci. USA 96: 12929–12934.

Clough, S.J. and Bent, A.F. 1998. Floral dip: a simplified method for *Agrobacterium*-mediated transformation of *Arabidopsis thaliana* . Plant J. 16: 735–743.

Cormack, B.P., Valdivia, R.H. and Falkow, S. 1996. FACS-optimized mutants of the green fluorescent protein (GFP). Gene 173: 33–38.

Cutler, S.R., Ehrhardt, D.W., Griffitts, J.S. and Somerville, C.R. 2000. Random GFP::cDNA fusions enable visualization of subcellular structures in cells of *Arabidopsis* at a high frequency. Proc. Natl. Acad. Sci. 97: 3718–3723.

Davidson, S.E., Smith, J.J., Helliwell, C.A., Poole, A.T. and Reid, J.B. 2004. The pea gene *LH* encodes *ent*-kaurene oxidase. Plant Physiol. 134: 1123–1134.

Dean, J.V., Shah, R.P. and Mohammed, L.A. 2003. Formation and vacuolar localization of salicylic acid glucose conjugates in soybean cell suspension cultures. Physiol. Plant. 118: 328–336.

Emanuelsson, O., Nielsen, H. and von Heijne, G. 1999. ChloroP, a neural network-based method for predicting chloroplast transit peptides and their cleavage sites. Protein Sci.: 978–984.

Fleet, C.M., Yamaguchi, S., Hanada, A., Kawaide, H., David, C.J., Kamiya, Y. and Sun, T.P. 2003. Overexpression of *AtCPS* and *AtKS* in Arabidopsis confers increased *ent*-kaurene production but no increase in bioactive gibberellins. Plant Physiol. 132: 830–839.

Grebenok, R.J., Pierson, E., Lambert, G.M., Gong, F.-C., Alfonso, C.L., Haldeman-Cahill, R., Carrington, J.C. and Galbraith, D.W. 1997. Green-fluorescent protein fusions for efficient characterization of nuclear targeting. Plant J. 11: 573–586.

Gregersen, S., Jeppesen, P.B., Holst, J.J. and Hermansen, K. 2004. Antihyperglycemic effects of stevioside in type 2 diabetic subjects. Metabolism 53: 73–76.

Haasen, D., Kohler, C., Neuhaus, G. and Merkle, T. 1999. Nuclear export of proteins in plants: AtXPO1 is the export receptor for leucine-rich nuclear export signals in *Arabidopsis thaliana* . Plant J. 20: 695–705.

Hansen, K.S., Kristensen, C., Tattersall, D.B., Jones, P.R., Olsen, C.E., Bak, S. and Møller, B.L. 2003. The in vitro substrate regiospecificity of recombinant UGT85B1, the cyanohydrin glucosyltransferase from *Sorghum bicolor*. Phytochemistry 64: 143–151.

Hedden, P. and Phillips, A.L. 2000. Gibberellin metabolism: new insights revealed by the genes. Trends Plant Sci. 5: 523–530.

Helliwell, C.A., Olive, M.R., Gebbie, L., Forster, R., Peacock, W.J. and Dennis, E.S. 2000. Isolation of an *ent*-kaurene oxidase cDNA From *Cucurbita maxima*. Aust. J. Plant Physiol. 27: 1141–1149.

Helliwell, C.A., Sheldon, C.C., Olive, M.R., Walker, A.R., Zeevaart, J.A.D., Peacock, W.J. and Dennis, E.S. 1998. Cloning of the *Arabidopsis ent*-kaurene oxidase gene GA3. Proc. Natl. Acad. Sci. USA 95: 9019–9024.

Helliwell, C.A., Sullivan, J.A., Mould, R.M., Gray, J.C., Peacock, W.J. and Dennis, E.S. 2001. A plastid envelope location of Arabidopsis *ent*-kaurene oxidase links the plastid and endoplasmic reticulum steps of the gibberellin biosynthesis pathway. Plant J. 28: 201–208.

Hofmann, K. and Stoffel, W. 1993. TMbase – a database of membrane spanning proteins segments. Biol. Chem. Hoppe-Seyle 374: 166.

Hsieh, M.H., Chan, P., Sue, Y.M., Liu, J.C., Liang, T.H., Huang, T.Y., Tomlinson, B., Chow, M.S., Kao, P.F. and Chen, Y.J. 2003. Efficacy and tolerability of oral stevioside in patients with mild essential hypertension: a two-year, randomized, placebo-controlled study. Clin. Ther. 25: 2797–2808.

Itoh, H., Tatsumi, T., Sakamoto, T., Otomo, K., Toyomasu, T., Kitano, H., Ashikari, M., Ichihara, S. and Matsuoka, M. 2004. A rice semi-dwarf gene, *Tan-Ginbozu* (d35), encodes the gibberellin biosynthesis enzyme, *ent*-kaurene oxidase. Plant Mol. Biol. 54: 533–547.

Kalinowska, M. and Wojciechowski, Z.A. 1987. Subcellular localization of UDPG nuatigenin glucosyltransferase in oat leaves. Phytochemistry 26: 353–358.

Kim, K.K., Sawa, Y. and Shibata, H. 1996. Hydroxylation of *ent*-kaurenoic acid to steviol in *Stevia rebaudiana* Bertoni – purification and partial characterization of the enzyme. Arch. Biochem. Biophys. 332: 223–230.

Kristensen, C., Morant, M., Olsen, C.E., Ekstrøm, C.T., Galbraith, D.W., Møller, B.L. and Bak, S. 2005. Metabolic engineering of dhurrin in transgenic *Arabidopsis* plants with marginal inadvertent effects on the metabolome and transcriptome. Proc Natl Acad Sci 102: 1779–1784.

Krogh, A., Larsson, B., von Heijne, G. and Sonnhammer, E.L. 2001. Predicting transmembrane protein topology with a hidden Markov model: application to complete genomes. J. Mol. Biol. 305: 567–580.

Kudo, N., Wolff, B., Sekimoto, T., Schreiner, E.P., Yoneda, Y., Yanagida, M., Horinouchi, S. and Yoshida, M. 1998. Leptomycin B inhibition of signal-mediated nuclear export by direct binding to CRM1. Exp. Cell Res. 242: 540–547.

Lim, E.K., Higgins, G.S., Li, Yi and Bowles, D.J. 2003. Regioselectivity of glucosylation of caffeic acid by a UDP-glucose:glucosyltransferase is maintained *in planta*. Biochem. J. 373: 987–992.

Liu, C.-J., Huhman, D., Sumner, L. and Dixon, R.A. 2003. Regiospecific hydroxylation of isoflavones by cytochrome P450 81E1 enzymes from *Medicago truncatula*. Plant J. 36: 471–484.

Loffelhardt, W. and Kopp, B. 1981. Subcellular localization of glucosyl transferases involved in cardiac glycoside glucosylation in leaves of *Convallaria majalis*. Phytochemistry 20: 1219–1222.

Minami, Y., Nishimura, O., Hara-Nishimura, I., Nishimura, M. and Matsubara, H. 2000. Tissue and intracellular localization of indican and the purification and characterization of indican synthase from indigo plants. Plant Cell Physiol. 41: 218–225.

Nagatani, A. and Matsushita, T. 2002. Light-induced nuclear targeting of phytochromeB-s green fluorescent protein in plants. In: B.W. Hicks (Ed.) Green Fluorescent Protein: Applications and Protocols, Humana Press, New Jersey.

Nakai, K. and Horton, P. 1999. PSORT: a program for detecting sorting signals in proteins and predicting their subcellular localization. Trends Biochem. Sci. 24: 34–36.

Neilsen, K.A. and Møller, B.L. 2005. Cytochrome P450s in plants. In: P.R. Ortiz Montellano (Ed.) Cytochrome P450: Structure, Mechanism and Biochemistry , 3rd edn., Kluwer Academic/Plenum Publishers, Dordrecht, pp. 553–584.

Rasmussen, S. and Dixon, R.A. 1999. Transgene-mediated and elicitor-induced perturbation of metabolic channeling at the entry point into the phenylpropanoid pathway. Plant Cell 11: 1537–1551.

Richman, A.S., Gijzen, M., Starratt, A.N., Yang, Z.-Y. and Brandle, J.E. 1999. Diterpene synthesis in *Stevia rebaudiana:* recruitment and up-regulation of key enzymes from the gibberellin biosynthetic pathway. Plant J. 19: 411–421.

Richman, A., Swanson, A., Humphrey, T., Chapman, R., McGarvey, B., Pocs, R. and Brandle, J. 2005. Functional genomics uncovers three glucosyltransferases involved in the synthesis of the major sweet glucosides of *Stevia rebaudiana*. Plant J. 41: 56–67.

Ro, D.K., Mah, N., Ellis, B.E. and Douglas, C.J. 2001. Functional characterization and subcellular localization of poplar (*Populus trichocarpa* × *Populus deltoides*) cinnamate 4-hydroxylase. Plant Physiol. 126: 317–329.

Sambrook, J. and Russell, D.W. 2001. Molecular Cloning: A Laboratory Manual., 3rd ed., Cold Spring Harbor Laboratory Press, Cold Spring Harbor.

Schmid, G., Hammer, D.K., Ritterbusch, A. and Grisebach, H. 1982. Appearance and immunohistochemical localization of UDP-glucose:coniferyl alcohol glucosyltransferase in spruce (*Picea abies*(L.) Karst.) seedlings. Planta 156: 207–212.

Schwab, W. 2003. Metabolome diversity: too few genes, too many metabolites?. Phytochemistry 62: 837–849.

Shibata, H., Sawa, Y., Oka, T., Sonoke, S., Kim, K.K. and Yoshioka, M. 1995. Steviol and steviol-glycoside: glucosyltransferase activities in *Stevia rebaudiana* Bertoni – purification and partial characterization. Arch. Biochem. Biophys. 321: 390–396.

Sun, T.P. and Kamiya, Y. 1994. The Arabidopsis *GA1* locus encodes the cyclase *ent*-kaurene synthetase A of gibberellin biosynthesis. Plant Cell 6: 1509–1518.

Wang, S.X. and Ellis, B.E. 1998. Enzymology of UDP-glucose: sinapic acid glucosyltransferase from *Brassica napus*. Phytochemistry 49: 307–318.

Warnecke, D.C. and Heinz, E. 1994. Purification of a membrane-bound UDP-glucose:sterol beta-D-glucosyltransferase based on its solubility in diethyl ether. Plant Physiol. 105: 1067–1073.

Werck-Reichhart, D., Bak, S. and Paquette, S. 2002. Cytochromes P450. In: C.R. Somerville (Ed.) The Arabidopsis Book, American Society of Plant Biologists, Rockville. doi/10.1199/tab.0009, http://www.aspb.org/publications/arabidopsis.

Yazaki, K., Inushima, K., Kataoka, M. and Tabata, M. 1995. Intracellular localization of UDPG: *p*-hydroxybenzoate glucosyltransferase and its reaction product in *Lithospermum* cell cultures. Phytochemistry 38: 1127–1130.

Ye, X., Al-Babili, S., Kloti, A., Zhang, J., Lucca, P., Beyer, P. and Potrykus, I. 2000. Engineering the provitamin A (beta-carotene) biosynthetic pathway into (carotenoid-free) rice endosperm. Science 287: 303–305.